Drones, quasi-spin or iso-spin? A comparison of many-body techniques for general spin

1976 J. Phys. A: Math. Gen. 9 187

(http://iopscience.iop.org/0305-4470/9/2/001)

J. Phys. A: Math. Gen., Vol. 9, No. 2, 1976. Printed in Great Britain.

Drones, quasi-spin or iso-spin? A comparison of many-body techniques for general spin

B J McKenzie and G E Stedman

Department of Physics, University of Canterbury, Christchurch, New Zealand

Received 18 June 1975

Abstract. For an effective-spin system with $2S+1$ levels there are a number of possible mappings of spin onto pseudo-fermion operators. We investigate the relative merits of three of these methods by calculating to second order the dispersion relation for coupled spin-phonon modes in crystals containing $S=1$ effective spin impurities. We find that the drone formalism quickly becomes intractable at higher spin values, as does the related quasi-spin formalism we develop, in contrast with the iso-spin (or Abrikosov projection) formalism.

1. Introduction

The success experienced in the application of the methods of quantum field theory to many-body physics (e.g. see Abrikosov *et al* 1963) is less marked in the field of spin or effective-spin systems (e.g. systems with discrete excitation levels) because of the greater complexity of the rules required. This arises because the spins do not obey either fermion or boson commutation relations and thus the fermion or boson Wick's theorems as such do not apply.

To overcome this difficulty, a number of approaches involving mappings of the spins onto fermion (or boson) operators has evolved. These in general allow Wick's theorem to be recovered at the expense of suitable operations to remove unphysical states that may arise.

We discuss three such mappings which are the simplest known to us (table 1). In each case S obeys spin, and $a_{j\mu}$, $b_{j\mu}$ fermion, commutation rules.

The *iso-spin* mapping, requiring just one fermion, was valuable in nuclear and particle physics (Lipkin 1965). It was introduced to many-body theory by Abrikosov (1965); for later work on the formalism see Oppermann (1973), Verwoerd (1974) and

Table 1. Spin-fermion mappings. μ ranges from $-S$ to $+S$ for iso-spin and 1 to $2S$ for drones and quasi-spin; $\mathcal{S}=[S(S+1)-\mu(\mu+1)]^{1/2}$; $S^{-}\equiv(S^{+})^{+}$.

	Iso-spin	Drone	Quasi-spin
S_j^z	$\sum_\mu \mu a_{j\mu}^+ a_{j\mu}$	$\sum_\mu (a_{j\mu}^+ a_{j\mu} - \frac{1}{2})$	$\sum_\mu \frac{1}{2}(a_{j\mu}^+ a_{j\mu} + b_{j\mu}^+ b_{j\mu} - 1)$
S_j^+	$\sum_\mu \mathcal{S} a_{j\mu+1}^+ a_{j\mu}$	$\sum_\mu a_{j\mu}^+ (b_{j\mu} + b_{j\mu}^+)$	$\sum_\mu a_{j\mu}^+ b_{j\mu}^+$

references therein. Unphysical states (in the fermion Fock space) may be removed by extending Abrikosov's projection method (see § 2).

The *drone* formalism was introduced by Mattis (1965) and generalized by Spencer (1968) and Barnes (1972). For applications, especially to coupled spin–phonon systems, see Toombs and Sheard (1973) and their references.

The *quasi-spin* mapping (Lipkin 1965) has not previously been used to generate a diagram technique for spin systems. It arises in superconductivity (Anderson 1958), atomic physics (Judd 1967) and crystal field theory (Wybourne 1973). In § 2, we develop the diagram method for general spin, using Barnes' (1972) formulation for drones as a guide.

In the following sections we discuss violation of the linked cluster theorem and calculation of $S = 1$ spin–phonon modes for all methods, concluding that in general the Abrikosov method is preferable to either drones or quasi-spin for $S > \frac{1}{2}$.

2. Formalism for general spin

Barnes' (1972) contribution to generalizing the drone method was to recognize that an arbitrary physical spin-space may be written as a direct sum of product drone–fermion spaces. This enabled him to find the trace over the spin states of an arbitrary spin operator in terms of traces over the product spaces multiplied by suitable factors to correct for the unphysical states. Finally he was able to show that if one used a diagram approach, the diagram value for arbitrary spin could be obtained by multiplying the appropriate $S = \frac{1}{2}$ diagram by a number of factors $K_S(l)$ where l is the number of drone–fermion loops labelled with the same site label. We now give a parallel analysis of quasi-spin.

For quasi-spin the operators for $S = \frac{1}{2}$ at a specific site (a_1^+, a_1, b_1^+, b_1) generate a two-dimensional space spanned by basis vectors $|11\rangle, |10\rangle, |01\rangle, |00\rangle$ where the first and second labels give the eigenvalues of the number operators $a_1^+ a_1, b_1^+ b_1$ respectively. Now by considering the operation of S^z, S^2 expressed in terms of the fermion operators acting on these basis vectors, one finds that $|11\rangle$, $|00\rangle$ correspond to $|S = \frac{1}{2}\, M_S = \frac{1}{2}\rangle$, $|S = \frac{1}{2}\, M_S = -\frac{1}{2}\rangle$ respectively and both $|10\rangle$, $|01\rangle$ correspond to $|S = 0\, M_S = 0\rangle$. Thus the fermion space contains *one* spin $\frac{1}{2}$ subspace and *two* spin zero subspaces. We write this as $\tilde{S}_{1/2} = S_{1/2} \oplus 2S_0$, where the tilde refers to the fermion space representation. Following Barnes, we find the spin states contained in any product space $(\otimes \tilde{S}_{1/2})^n$ and by inverting these, we obtain the physical spin spaces as a direct sum of fermion spaces. For example:

$$S_{1/2} = (\otimes \tilde{S}_{1/2})^1 \ominus 2S_0$$

$$S_1 = (\otimes \tilde{S}_{1/2})^2 \ominus 4(\otimes \tilde{S}_{1/2})^1 \oplus 3S_0$$

$$S_{3/2} = (\otimes \tilde{S}_{1/2})^3 \ominus 6(\otimes \tilde{S}_{1/2})^2 \oplus 10(\otimes \tilde{S}_{1/2})^1 \ominus 8S_0$$

with the notation $(\otimes \tilde{S}_{1/2})^2 = \tilde{S}_{1/2} \otimes \tilde{S}_{1/2}$ etc.

One obtains for an arbitrary spin operator θ,

$$\langle\theta\rangle_{S=1/2} = Y_{1/2}(1)\langle\theta\rangle_{\tilde{1}}$$

$$\langle\theta\rangle_{S=1} = Y_1(2)\langle\theta\rangle_{\tilde{2}} - 4\,Y_1(1)\langle\theta\rangle_{\tilde{1}}$$

etc, where $\langle\theta\rangle_{S=1}, \langle\theta\rangle_{\tilde{n}}$ denote the unperturbed thermal average of θ with respect to the

spin 1 states and the states of the nth-fermion product space $(\otimes \tilde{S}_{1/2})^n$ respectively, and

$$Y_S(n) = \mathrm{Tr}_{\tilde{n}} \exp(-\beta \mathscr{H}_S)/\mathrm{Tr}_S \exp(-\beta \mathscr{H}_S).$$

If the zero-order spin Hamiltonian has the form $\mathscr{H}_S = \omega_0 \Sigma_j S_j^z$, the multiplicative factors are $Y_S(n) = [(f^+ f^-)^n Z_S]^{-1}$ with $f^\pm = [1 + \exp(\pm \beta\omega_0/2)]^{-1}$ and where Z_S is the true partition function for the S spin state.

The value of the Feynman diagram corresponding to arbitrary spin S is to be evaluated by multiplying the value of the corresponding $S = \frac{1}{2}$ diagram by suitable factors:

$$\langle \text{diagram} \rangle_S = K_S(l, p) K_S(m, q) \ldots \langle \text{diagram} \rangle_{S=1/2}$$

where, for each diagram involving several sites, there is a factor $K_S(l, p)$ for each distinct site with l loops and p 'free' spin-state labels. For example $K_1(l, p) = Y_1(2) l^p - 4 Y_1(1)$. We shall find that, for certain diagrams, p is not necessarily equal to the power of the product space as stated by Barnes.

In the Abrikosov formalism, the approach for removing the effect of unphysical states is somewhat different. Because the spaces considered here are not powers of $S = \frac{1}{2}$ spaces one cannot apply a method like that used for drones and quasi-spin except for the case $S = \frac{1}{2}$. (This is effectively the approach of Yolin (1965) when he multiplies his diagrams by a factor $Y^p = [(1 + \cosh \beta\omega_0)/\cosh \beta\omega_0]^p$, where p is the number of distinct spins represented in the diagram.) The conventional approach is to add an energy λ to each fermion and then remove the effect of the unphysical multiparticle states at the end of the calculation by means of the projection

$$\boldsymbol{P} = \frac{1}{\mathrm{Tr} \exp(-\beta \mathscr{H}_S)} \lim_{\lambda \to \infty} \mathrm{e}^{\beta\lambda}. \tag{1}$$

3. Linked cluster theorem

Keiter (1968, 1971) pointed out that the Abrikosov 'freezing-out' procedure (equation (1)) destroys the linked cluster theorem (LCT). We express this by

$$\mathscr{D} = \mathscr{D}^0 + \frac{\boldsymbol{P}\{C\} + \boldsymbol{P}\{CD\}}{1 + \boldsymbol{P}\{D\}} \tag{2}$$

where $\mathscr{D}, \mathscr{D}^0$ are the perturbed and unperturbed phonon propagators respectively. C represents the connected diagrams with the exception of $\mathscr{D}^0$ and D the vacuum diagrams with the exception of 1.

Equation (2) is also valid for drones and quasi-spin with the exception that $\boldsymbol{P}$ now has the significance of multiplying the diagram by the appropriate $K_S(l, p)$ factors. The LCT fails in these cases also because the factors multiplying the disconnected diagrams (e.g. CD) do not factorize into the parts that multiply the corresponding connected (C) and vacuum (D) diagrams.

In a weak-coupling problem such as the spin–phonon coupled-modes problem to be considered in § 4, $(1 + \boldsymbol{P}\{D\})^{-1}$ can be expanded using the binomial theorem. Because the diagram factors do not factorize appropriately, the disconnected diagrams that result (e.g. $\boldsymbol{P}\{CD\} - \boldsymbol{P}\{C\} \,.\, \boldsymbol{P}\{D\}$) do not cancel. As an example of this, consider the approach of Yolin (1965) who was criticized by Schultz and Kwok (1972) for assuming

LCT. As we have already mentioned, dealing with the Abrikosov technique for $S=\frac{1}{2}$ enabled Yolin to remove the effect of unphysical states by multiplying his diagrams by a factor Y^p. The first disconnected diagram to appear in the expansion arises in the fourth order and is indicated in figure 1 (using Yolin's conventions). Although the similar diagrams with $n_1 \neq n_2$ cancel, the one with $n_1 = n_2$ does not, and must be multiplied by a factor $(Y - Y^2)$; Yolin in his work presumably did not realize this. However, the diagram does not affect his calculation of the lifetime of the coupled modes as it contributes no imaginary part, and thus his calculation agrees with other published results for the lifetime (e.g. see Toombs and Sheard 1973, Fidler and Tucker 1970). This diagram would affect only the fourth-order frequency shift.

In the case of drones, for $S=\frac{1}{2}$, the LCT is recovered; the $K_{1/2}(l, p)$ factors are all unity and hence the required factorization results.

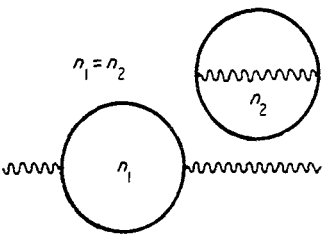

Figure 1. A fourth-order unlinked diagram arising in the problem of Yolin. Full lines represent A^0 propagators (equation (4)) and wavy lines the phonon propagator.

4. Example: spin–phonon coupled modes for $S=1$

The relative usefulness of the previous three methods for $S>\frac{1}{2}$ may be assessed by applying each to a specific problem, namely the coupled-modes dispersion relation for $S=1$.

Our model Hamiltonian is chosen as follows:

$$\mathcal{H} = \mathcal{H}_s + \mathcal{H}_p + \mathcal{H}_{sp}$$

$$\mathcal{H}_s = \omega_0 \sum_j S_j^z \qquad \mathcal{H}_p = \sum_k \omega_k c_k^+ c_k$$

$$\mathcal{H}_{sp} = N^{-1/2} \sum_{k,j} B_k \exp(i\boldsymbol{k}.\boldsymbol{R}_j)\psi_k[S_j^x + \xi(S_j^+ S_j^+ + S_j^- S_j^-)] \tag{3}$$

where $B_k = \frac{1}{2}\epsilon(\omega_0\omega_k)^{1/2}$ is the coupling coefficient and $\psi_k = c_k + c_{-k}^+$ is a lattice mode amplitude operator. The interaction term with coefficient ξ is required to enable a phonon mode to couple all second-order states (e.g. Fidler and Tucker 1971).

We require the poles of the perturbed phonon propagator defined (following Toombs and Sheard 1973, in their notation) by

$$D_{kk'}(\tau) = -\langle T_\tau\{\psi_k(\tau)\psi_{-k'}(0)\}\rangle.$$

The corresponding unperturbed phonon propagator has Fourier coefficients diagonal in k, k':

$$\mathscr{D}_k^0(i\omega_n) = \frac{2\omega_k}{(i\omega_n)^2 - \omega_k^2}.$$

For the procedures needed to develop a diagram expansion for $\mathscr{D}_k(i\omega_n)$ see Abrikosov *et al* (1963).

Below we evaluate the diagrams generated for the drone, quasi-spin and Abrikosov techniques individually.

4.1. *Drones*

We define propagators,

$$\begin{aligned} \Delta^0_{j\mu;j'\mu'}(\tau) &= -\langle T_\tau\{\phi_{j\mu}(\tau)\phi_{j'\mu'}(0)\}\rangle_0 \\ A^0_{j\mu;j'\mu'}(\tau) &= -\langle T_\tau\{a_{j\mu}(\tau)a^+_{j'\mu'}(0)\}\rangle_0 \end{aligned} \tag{4}$$

where $\phi_{j\mu} = b_{j\mu} + b^+_{j\mu}$, which have Fourier coefficients diagonal in μ, μ' and in j, j':

$$\Delta^0(i\omega_n) = 2/i\omega_n \qquad A^0(i\omega_n) = 1/(i\omega_n - \omega_0).$$

One obtains the second-order diagrams shown in figure 2 where the propagators $\mathscr{D}^0_k\Delta^0$ and A^0 are represented by wavy, broken and full lines respectively.

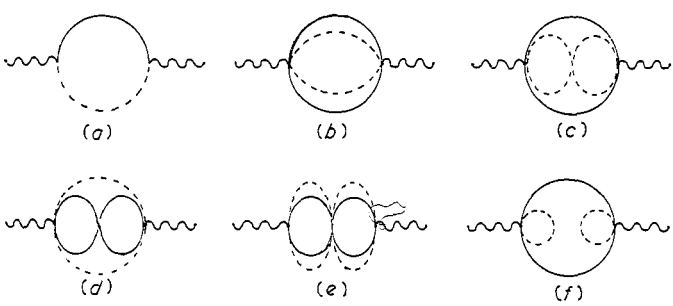

Figure 2. Second-order diagrams in the drone and quasi-spin formulation. Diagram (*f*) should be omitted for quasi-spin.

It is necessary to distinguish figures 2(*b*, *c*) in this manner because, although the diagrams themselves all have the same value, the $K_S(l, p)$ factors multiplying them are different both in magnitude and sign. This arises from the contraction of factors of the form

$$\sum_{j'}\sum_{\mu_1\mu_1'}\sum_{\mu_2\mu_2'} \langle T_\tau\{a_{j\mu_1}(\tau_1)\phi_{j\mu_1}(\tau_1)a_{j\mu_1'}(\tau_1)\phi_{j\mu_1'}(\tau_1)\phi_{j\mu_2'}(\tau_2)a_{j\mu_2'}(\tau_2)\phi_{j'\mu_2'}(\tau_2)a_{j'\mu_2'}(\tau_2)\}\rangle_0.$$

Depending on the pairs one chooses to contract, one can obtain products of Kronecker deltas like $\delta_{jj'}(\delta_{\mu_1\mu_2})^2(\delta_{\mu_1'\mu_2'})^2$ (figure 2 (*b*)), $\delta_{jj'}[\delta_{\mu_1\mu_2'}]^2[\delta_{\mu_1'\mu_2}]^2$ (figure 2(*e*)), which result in a single sum over j and a double sum over μ_1, μ_1'; or like $\delta_{jj'}\delta_{\mu_1\mu_2}\delta_{\mu_1'\mu_2}\delta_{\mu_1\mu_2'}\delta_{\mu_1'\mu_2}$ (figures 2(*c*, *d*)), which leave only single sums over j and μ. Thus figures 2(*b*, *e*) have

factors like $K_1(1,2)$ multiplying them while figures 2(*c*, *d*) have a factor $K_1(1,1)$ and also a different sign.

The diagram convention used in figure 2 is to label the outgoing stubs (μ_1, μ_1') and ingoing stubs (μ_2, μ_2') in the same order at each vertex (see figure 3), and introduce the twists to connect them. Evaluating the diagrams and their K factors, one obtains the contribution to $\mathscr{D}_k(i\omega_m)$ given in table 2.

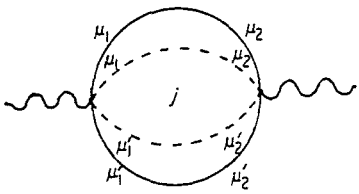

Figure 3. Labelling conventions for figure 2.

Table 2. Diagram contributions for drones. For brevity we define $G_\pm(\omega_0) = \exp(\beta\omega_0) \pm \exp(-\beta\omega_0)$, $H_\pm(\omega_0) = \exp(\beta\omega_0) \pm 1$, $I(\omega_0) = H_+(\omega_0)H_+(-\omega_0)$, $Z(\omega_0) = G_+(\omega_0)+1$.

Figure	Diagram	K factor
2(*a*)	$\dfrac{\frac{1}{2}\epsilon^2\omega_0^2\omega_k G_-(\omega_0)}{[(i\omega_m)^2-\omega_0^2]I(\omega_0)}$	$2\dfrac{I(\omega_0)}{Z(\omega_0)}$
2(*b*–*e*)	$\dfrac{\xi^2\epsilon^2\omega_0^2\omega_k}{(i\omega_m)^2-4\omega_0^2}\dfrac{G_+(\omega_0)H_-(2\omega_0)H_-(-\omega_0)}{G_-(\omega_0)H_+(2\omega_0)H_+(-\omega_0)}$	$-4\dfrac{I(\omega_0)}{Z(\omega_0)}$
2(*f*)	0	$2\dfrac{I(\omega_0)}{Z(\omega_0)}$

4.2. *Quasi-spin*

We define propagators $A^0_{j\mu;j'\mu'}(\tau)$ by equation (4) and also

$$E^0_{j\mu;j'\mu'}(\tau) = -\langle T_\tau\{b_{j\mu}(\tau)b^+_{j'\mu'}(0)\}\rangle_0.$$

Again the Fourier coefficients are diagonal in j and μ labels, but they have different values since $\mathscr{H}_s$ has a different fermion representation:

$$A^0(i\omega_n) = E^0(i\omega_n) = \frac{1}{i\omega_n - \omega_0/2}.$$

The diagrams obtained can again be represented by those of figure 2 except that the broken and full lines now represent the A^0 and E^0 propagators respectively, and figure 2(*f*) does not appear. The evaluated diagrams and their factors are given in table 3.

4.3. *Abrikosov*

We define the propagator $A_{j\mu,j'\mu'}(\tau)$ using equation (4). The corresponding unperturbed propagator has Fourier coefficients diagonal in j, j' and μ, μ', but now a function

Table 3. Diagram contributions for quasi-spin. Abbreviations are defined in the caption to table 2; $X \equiv \{[\exp(\frac{3}{2}\beta\omega_0) - \exp(-\omega_0/2)][\exp(\beta\omega_0) - \exp(-\frac{1}{2}\beta\omega_0)]\}/H_+(\frac{3}{2}\omega_0)$.

Figure	Diagram	K factor
2(*a*)	$\dfrac{-\frac{1}{2}\epsilon^2\omega_0^2\omega_k}{(i\omega_m)^2-\omega_0^2}\dfrac{G_-(\frac{1}{2}\omega_0)}{I(\frac{1}{2}\omega_0)}$	$-2\dfrac{I(\frac{1}{2}\omega_0)G_+(\frac{1}{2}\omega_0)}{Z(\omega_0)}$
2(*b–e*)	$\dfrac{+\xi^2\epsilon^2\omega_0^2\omega_k}{[(i\omega_m)^2-4\omega_0^2]}\dfrac{G_-(\frac{1}{2}\omega_0)X}{I(\frac{1}{2}\omega_0)H_+^2(-\frac{1}{2}\omega_0)H_-(\omega_0)}$	$-4\dfrac{I^2(\frac{1}{2}\omega_0)}{Z(\omega_0)}$

$d\mu$:

$$A_\mu^0(i\omega_n) = \frac{1}{i\omega_n - \mu\omega_0} \qquad \mu = 0, \pm 1. \tag{5}$$

If one adds energy λ to each fermion, $\mu\omega_0 \to \mu\omega_0 + \lambda$, in equation (5). One obtains the diagrams shown in figure 4 in which the propagators A_1^0, A_0^0 and A_{-1}^0 are represented by full lines above, on or below the level of the phonon propagator respectively. Figures 4(*a, b*) correspond to figure 2(*a*), and figure 4(*c*) corresponds to figures 2(*b–e*).

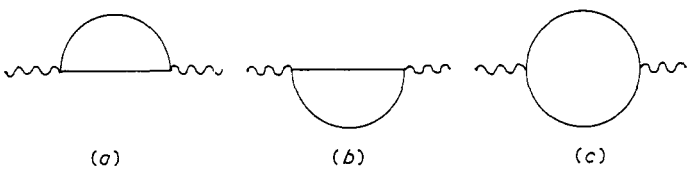

Figure 4. Diagrams for the Abrikosov formulation. Different orientations of the full line distinguish the A_μ^0 (see text).

Evaluating these but before having applied the limiting procedure of equation (1), we obtain

$$\begin{aligned} &\text{figures } 4(a, b): \quad \frac{\epsilon^2\omega_0^2\omega_k}{(i\omega_m)^2-\omega_0^2}U(\lambda) \\ &\text{figure } 4(c): \quad \frac{4\xi^2\epsilon^2\omega_0^2\omega_k}{(i\omega_m)^2-4\omega_0^2}U(\lambda) \end{aligned} \tag{6}$$

where $U(\lambda) = 1/[\exp(-\beta\omega_0)\exp(-\beta\lambda)+1] - 1/[\exp(\beta\omega_0)\exp(-\beta\lambda)+1]$. Applying the limiting procedure described in § 2 to the factor $U(\lambda)$ in equation (6), one obtains

$$Q(\omega_0) \equiv G_-(\omega_0)/Z(\omega_0) \tag{7}$$

precisely the factor obtained when the contributions from the diagrams and K factors in tables 2 and 3 are combined.

In § 5 we will explain why the method of § 4.3 (Abrikosov) is preferable to those of §§ 4.1 (drones) and 4.2 (quasi-spin). First we complete the derivation of the coupled-mode dispersion relation. Considering the second-order diagrams calculated as contributing to a self-energy $\Pi_k(i\omega_m)$

$$\mathcal{D}_k(i\omega_m) = \frac{1}{[\mathcal{D}_k^0(i\omega_m)]^{-1} - \Pi_k(i\omega_m)} \tag{8}$$

then $\mathscr{D}_k(i\omega_n)$ is given correct to second order. Thus, to second order,

$$\Pi_k(i\omega_m) = \epsilon^2\omega_0^2\omega_k Q(\omega_0)\left(\frac{1}{(i\omega_m)^2-\omega_0^2}+\frac{4\xi^2}{(i\omega_m)^2-4\omega_0^2}\right).$$

This is substituted into equation (8), $i\omega_m$ is analytically continued to ω, and then the poles are obtained by equating the denominator to zero. This gives

$$(x-y)(x-4)(x-1)-\epsilon^2 yQ(\omega_0)[(x-4)+4\xi^2(x-1)]=0 \tag{9}$$

where $x=(\omega/\omega_0)^2$, $y=(\omega_k/\omega_0)^2$. By obtaining the three roots of equation (9) for x as a function of y one obtains the dispersion curve for the coupled spins. In figure 5 curves are given for $\epsilon^2=0{\cdot}1$ and $\epsilon^2=0{\cdot}01$, with $\xi=1$ and with β chosen such that $Q(\omega_0)=1$.

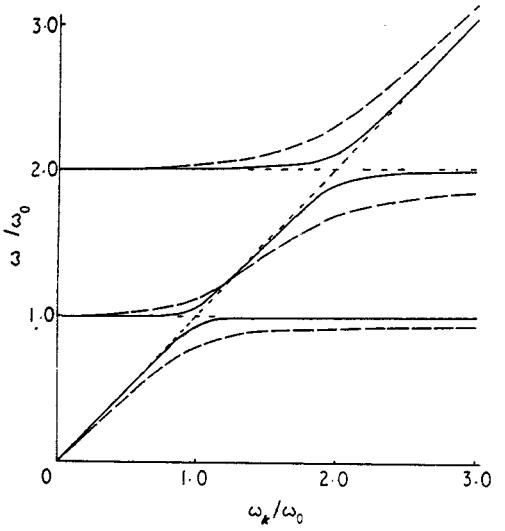

Figure 5. Coupled-mode dispersion relation for $S=1$, evaluated for two strengths of coupling. The full curve represents the solution for $\epsilon^2=0{\cdot}01$, and the broken curve for $\epsilon^2=0{\cdot}1$.

5. Comparison of techniques

The main advantage of using the Abrikosov technique is that, in the evaluation of figure 4(*c*), only one integration is required. The equivalent diagrams for drones and quasi-spin (figures 2(*b–e*)) require three nested integrations. For general S, the Abrikosov approach would yield $S(2S+1)$ diagrams, each requiring one integration; the drone or quasi-spin technique would give $2S$ diagrams, but a number of free integration variables ranging from 1 (for the first diagram) to $4S-1$ (for the last). The Abrikosov technique also avoids the necessity of differentiating the diagrams (and the K factors) in figures 2(*b–e*). If one took a perturbation linear in spin ($\xi=0$ in equation (3)) these comments would not apply, and the three methods would be comparable; however this choice of interaction is less realistic for general spin in the physical problems we have in mind.

The standard basis operator technique of Yang and Wang (1974) could be a serious competitor to the Abrikosov method at higher spin values. However, this method is much different in structure to the methods considered in this paper.

We conclude that although drones, quasi-spin and Abrikosov projection techniques are comparable for $S=\frac{1}{2}$, the first two methods quickly become intractable with increasing spin for realistic choices of the interaction Hamiltonian, and the advantages of the Abrikosov technique render it the most attractive method.

Acknowledgment

B J McKenzie is grateful to the New Zealand University Grants Committee for a Postgraduate Scholarship.

References

Abrikosov A A 1965 *Physics* **2** 5–20
Abrikosov A A, Gor'kov L P and Dzyaloshinskii I Y 1963 *Methods of Quantum Field Theory in Statistical Physics*, 2nd edn (Oxford: Pergamon Press)
Anderson P W 1958 *Phys. Rev.* **112** 1900–16
Barnes S E 1972 *J. Phys.* C: *Solid St. Phys.* **5** L178–80
Fidler F B and Tucker J W 1970 *Solid St. Commun.* **8** 2055–8
—1971 *J. Phys.* C: *Solid St. Phys.* **4** 2583–92
Judd B R 1967 *Second Quantization and Atomic Spectroscopy* (Baltimore: Johns Hopkins) p 41
Keiter H 1968 *Z. Phys.* **213** 466–81
—1971 *Phys. Lett.* **36A** 257
Lipkin H J 1965 *Lie Groups for Pedestrians* (Amsterdam: North Holland)
Mattis D C 1965 *Theory of Magnetism* (New York: Harper and Row)
Oppermann R 1973 *Z. Phys.* **259** 285–300
Schultz T D and Kwok P C 1972 *Phys. Lett.* **39A** 402–4
Spencer H J 1968 *Phys. Rev.* **167** 430–3
Toombs G A and Sheard F W 1973 *J. Phys.* C: *Solid St. Phys.* **6** 1467–88
Verwoerd W S 1974 *Phys. Rev.* B **10** 2868–82
Wybourne B G 1973 *Int. J. Quantum Chem.* **7** 1117–37
Yang D H and Wang Y 1974 *Phys. Rev.* B **10** 4714–23
Yotin E M 1965 *Proc. Phys. Soc.* **85** 759–65